EFFECTS OF Zn CONTENT ON THE MICROSTRUCTURE AND PROPERTIES OF Al-12.5Si-xZn-2Cu-Mg ALLOY

Rui Guo, Jiangang He, Fengguang Li, Qiuyue Shi and Daxin Zeng
College of Materials Engineering, Hubei University of Automotive Technology, Shiyan 442002, Hubei Province, China

https://doi.org/10.1007/s40962-022-00942-2

Abstract

Zn has been added to the Al-12.5wt%Si-2wt%Cu-1wt%Mg (abbrev Al-12.5Si-2Cu-Mg) alloy. By utilizing optical microscope (OM), X-ray diffraction (XRD), and scanning electron microscope (SEM), the microstructure and phase structure of the alloy were investigated. The alloy's mechanical properties and wear resistance were evaluated. The results demonstrate that the as-cast microstructure of Al-12.5Si-xZn-2Cu-1Mg alloy consists of (α-Al + Si) eutectic, a minor amount of primary Si, θ-Al_2Cu phase, Q-$Al_5Cu_2Mg_8Si_6$ phase, and π-$Al_8Mg_3FeSi_6$ phase. In the final solidification zone of an alloy with a Zn content greater than 2%, a Zn-rich granular phase is observed. With an increase in Zn content, the size of the Si phase decreases and the number of θ-Al_2Cu phase decreases. Zn slightly raises the formation temperature of primary Si, decreases the (α-Al + Si) eutectic transition temperature, and significantly decreases the formation temperatures of θ-Al_2Cu and Q-$Al_5Cu_2Mg_8Si_6$ phases. The yield strength and hardness of the as-cast alloy raise with increasing Zn content, whereas the elongation decreases and the tensile strength first increases and then decreases slightly. The tensile strength is the greatest when the weight percentage of Zn is 2wt%. After T6 treatment, the tensile strength, yield strength, and hardness of the alloy rise in proportion to the alloy's Zn content, and its resistance to wear is greatly enhanced.

Keywords: *Al-Si-Zn-Cu-Mg alloy, microstructure, alloy properties*

Introduction

Al-Si cast alloys have the advantages of good casting performance, good wear resistance and low linear expansion rate.[1–4] After adding Cu, Mg and other elements, they can be strengthened by heat treatment to achieve greater strength. They are utilized extensively in the automobile, manufacturing, aerospace and other industrial areas.[5–7] Zn is an important strengthening element in some aluminum alloy materials. Zn can be dissolved in α-Al and play a certain solid solution strengthening role.[8] Zn forms a strengthening phase in the multi-element alloy with Cu, Mg and other elements, which can significantly improve the strength of aluminum alloy.[9] However, studies on the role of Zn in the Al-Si-Cu-Mg alloy are limited.[10–12] Zhang et al. investigated the influence of Zn on the microstructure and properties of cast Al-Si-Cu-Mg alloy, and found that Zn can improve the aging hardness of the alloy, but when the Zn content exceeds 1wt%, the hardness drops.[13] Nemri et al. studied the effect of Zn on the microstructure and mechanical properties of the Al-11Si-2Cu-0.1Mg alloy.[14] It was found that Zn had no effect on the dendrite structure and eutectic Si morphology of the as-cast alloy. When Zn was added at a 0.4 wt% weight percent, the strength was reduced. When the amount of Zn added was between 1.5 wt% and 3.11 wt%, the effect on mechanical properties was insignificant. Y Alemdag et al. discovered that Zn promoted the increase of the Si phase in the Al-12Si-3Cu alloy, and Zn content less than 2 wt% enhanced the mechanical properties and wear resistance of the alloy.[15]

There is little research on the influence of Zn content on eutectic Al-Si-Cu-Mg cast alloy, although Zn has been studied as a strengthening element in Al-Si-Cu-Mg alloy. In addition, the EN AC-AlSi12CuNiMg cast aluminum alloy in the European standard EN 1706 shows high strength and wear resistance as a piston material for internal combustion engines. However, Ni element is a costly additive element to improve high temperature

Received: 21 September 2022 / Accepted: 09 December 2022 / Published online: 5 January 2023

performance, so Zn element is expected to be a potential alternative reinforcement element. The purpose of this research is to investigate the effect of Zn content on the microstructure and properties of Al-12.5Si-2Cu-Mg alloy in order to develop cast aluminum alloy materials with high strength and high wear resistance.

Experimental Details

Al-12.5Si-2Cu-Mg-(0-4) Zn alloy was prepared by melting Al-7Si alloy in a crucible at 700 °C. When the alloy was molten, crystalline silicon and electrolytic copper were added, and the crystalline silicon was completely pressed into the aluminum liquid to ensure complete dissolving. And then, pure magnesium was dipped into the aluminum liquid and stirred carefully to melt it. When the charge is entirely melted, the temperature is raised to 780°C for 30 minutes, and the 0.4 wt% Cu-9P is added. After the treatment, the temperature of the liquid alloy was lowered to 750°C and 1.2 wt% $MnCl_2$ was added as a refining agent. Lastly, the aluminum sodium-free slag agent was applied to the surface of the molten aluminum. After 10-15 minutes of stirring and standing, the slag was removed to obtain the aluminum alloy melt. The metal mold (displayed in Figure 1a) samples were prepared when the metal mold's preheating temperature was 240°C ± 5°C, and its pouring temperature was 750°C ± 5°C. The alloy's cooling curve was recorded using the sample cup for thermal analysis depicted in Figure 1b. The samples were heat-treated by the T6 process. After 8 hours of solution treatment at 510°C, the samples were immediately quenched in water at 20 ± 5°C, aged for 4 hours at 170°C, and then cooled in a furnace.

The composition of the alloy was examined using a spectrometer with direct reading. For microstructure observation, the same position of alloy samples with varied compositions was used. The samples were polished with sandpaper ranging from 180 to 2000 grit. After washing, they were etched for approximately 7 seconds in a 0.5 wt% HF alcohol solution. The optical microscope was used to characterize the metallographic structure, while the JSM-6510LV field emission scanning electron microscope (SEM) was used to analyze the fracture morphology, microstructure, and energy spectrum. Image Pro Plus (IPP) software is utilized to measure the average size of the Si phase in the alloy structure. A DX-2700 Cu target X-ray diffractometer was utilized for phase analysis with the sample having the dimensions of 10x10x5mm after grinding and leveling. The scanning range was from 10° to 90°, while the scanning speed was 0.02 °/s. Brinell hardness was measured by Brinell hardness tester with a φ5 mm indenter, 250 kg applied load, and 30s holding time. The average hardness value of 5 points on each sample was taken as the material hardness value. As depicted in Figure 2, the as-cast metal mold sample was utilized for the tensile test according to the national standard GB/T 1173-2013. The loading speed on the universal testing machine was 0.2 mm/s. As the test result for each condition, the mean value of the three samples was picked, and the elongation of the tensile sample was calculated by measuring the gauge length of the broken sample.

The wear resistance test was conducted using the MMX-3G multifunctional friction and wear tester. The disk-pin grinding method was applied. The material of the grinding disk was quenched 45 steel with a size of φ31.7 mm x10 mm. The Al-12.5Si-2Cu-Mg- (0-4) Zn alloy, after T6 heat treatment, was machined into a pin of φ4.8 mm x 12.7 mm.

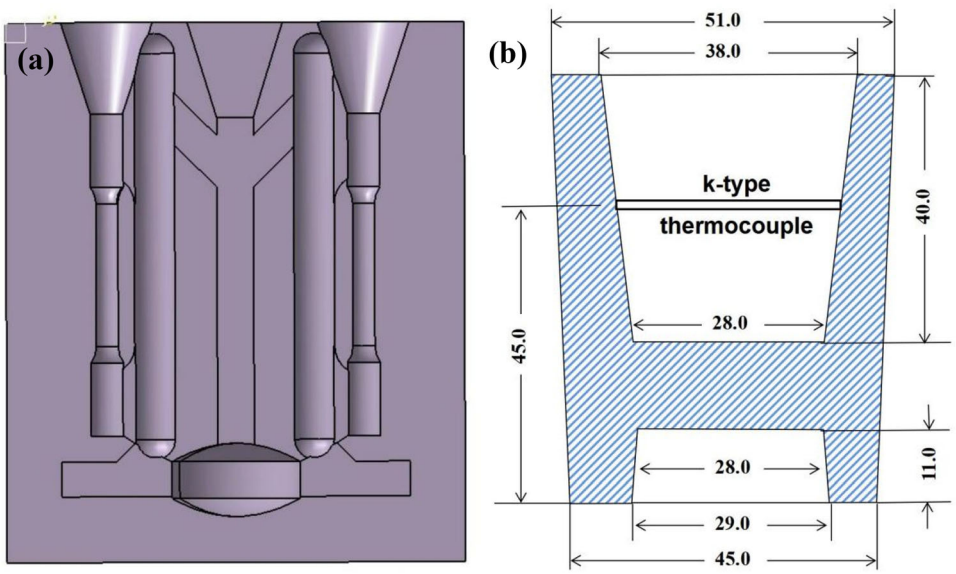

Figure 1. Schematic diagram of metal die section (a) and sample cup for thermal analysis (b).

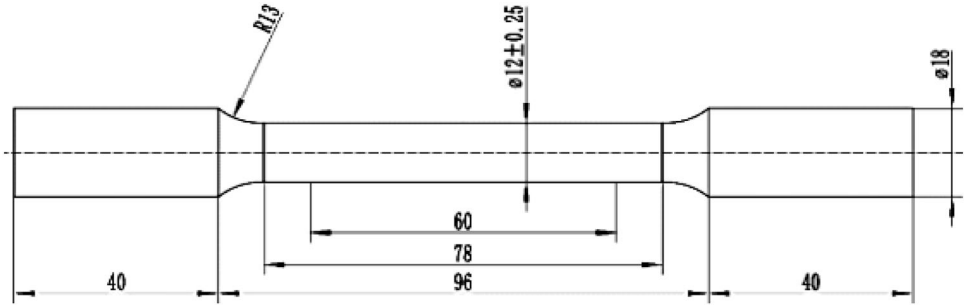

Figure 2. Illustration of a tensile specimen.

The test was performed under dry friction conditions with a 30N load, 200 r/min rotational speed, and 60min friction time. After ultrasonic cleaning, the measured sample was weighed to calculate the weight loss of the sample during the wear process, and the SEM was used to characterize the surface of the wear sample.

Experimental Results

After spectral analysis, the chemical composition of as-cast Al-12.5Si-2Cu-Mg- (0-4) Zn alloys is shown in Table 1. It can be seen that the as-cast alloy's composition is basically consistent with the design composition.

Effect of Zn Content on the Microstructure of Al-12.5Si-2Cu-Mg- (0-4) Zn Alloy

Figure 3 depicts the metallographic structure of alloys with varying Zn content. The microstructure of alloys with varying Zn contents is composed of α-Al, short-flake eutectic Si, and fine-block primary Si phase, as depicted in the picture. There is no obvious α-Al dendrite and the Si phase is evenly distributed. However, with the increase of Zn content in the alloy, the proportion of primary Si phase increases.

Table 1. The Measured Composition of Alloys with Different Zn Content (Mass Fraction/%)

Item	Si	Cu	Mg	Zn	Mn	Fe	Al
Al-12.5Si-2Cu-1Mg	12.39	1.92	0.97	–	0.26	0.09	Bal.
Al-12.5Si-1Zn-2Cu-1Mg	12.31	1.95	0.95	0.96	0.26	0.10	Bal.
Al-12.5Si-2Zn-2Cu-1Mg	12.34	1.94	0.97	1.93	0.26	0.09	Bal.
Al-12.5Si-3Zn-2Cu-1Mg	12.31	2.00	0.94	3.01	0.26	0.09	Bal.
Al-12.5Si-4Zn-2Cu-1Mg	12.41	1.96	0.99	4.04	0.26	0.08	Bal.

Al-Si-Cu-Mg alloy phase composition contains in addition to α-Al and Si, but also the existence of θ-Al_2Cu phase, Q-$Al_5Cu_2Mg_8Si_6$ phase and iron-rich phase π-$Al_8Mg_3FeSi_6$ compound phase.[4] Because these compound phase sizes are not displayed in the optical metallographic photograph, which will be discussed later.

Effect of Zn on Si Phase in Alloy

The grain size of the Si phase in the alloy was measured by IPP software, and the results are depicted in Figure 4. The results indicate that the size of the Si phase in the alloy without Zn addition is large, mainly concentrated in the region of 30 to 45 μm, and the average size of the Si phase is 37.5 μm. With the increase of Zn content, the Si phase in the alloy becomes more refined. When the addition amount is 2 wt%, the average size of the eutectic silicon phase Si phase is reduced to 29.5 μm, the Zn content in the alloy increases, and there is no noticeable refinement of the Si phase.

Compound Phase in Alloy

Figure 5 shows the XRD pattern of Al-12.5Si-2Cu-1Mg, Al-12.5Si-2Zn-2Cu-1Mg and Al-12.5Si-4Zn-2Cu-1Mg alloys. It can be observed that the diffraction peaks of the three alloys correspond to the three phases of α-Al, Si and θ-Al_2Cu and are absolutely similar.

Figure 6 shows the SEM images of as-cast alloy samples with different Zn contents, as well as surface scanning images of EDS elements. It can be evidenced that compared with the addition of Zn element, the Si, Mg and Cu elements in the as-cast structure have enrichment regions, while the distribution of Zn element is relatively uniform, and there is no obvious enrichment phenomenon, which indicates that there are compound phases formed by Si, Mg

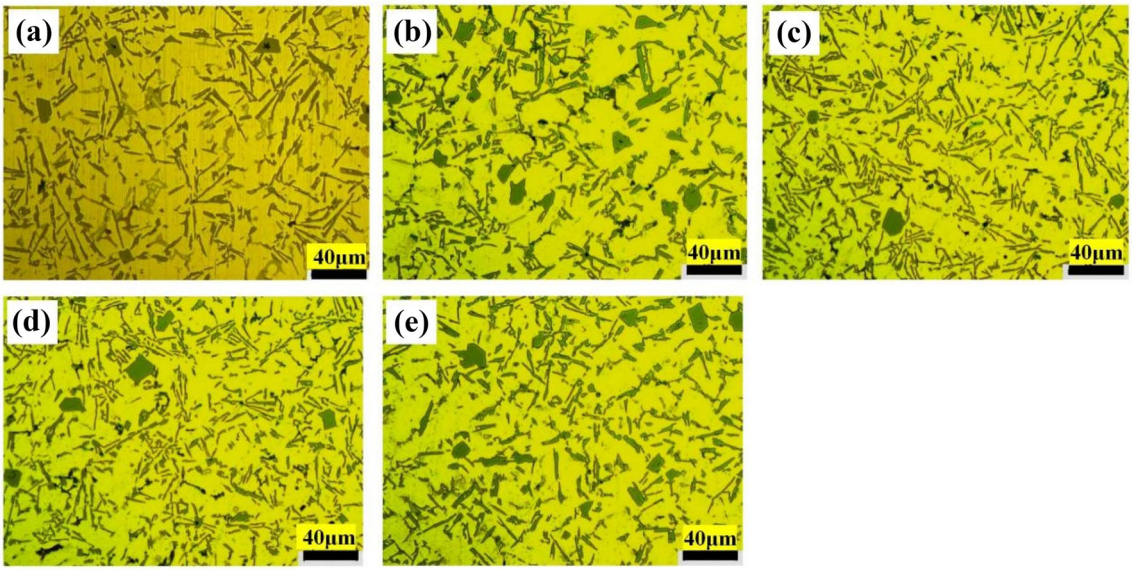

Figure 3. Metallographic structure of alloys with different Zn content (a) Al-12.5Si-2Cu-1Mg; (b) Al-12.5Si-1Zn-2Cu-1Mg; (c) Al-12.5Si-2Zn-2Cu-1Mg; (d) Al-12.5Si-3Zn-2Cu-1Mg; (e) Al-12.5Si-4Zn-2Cu-1Mg.

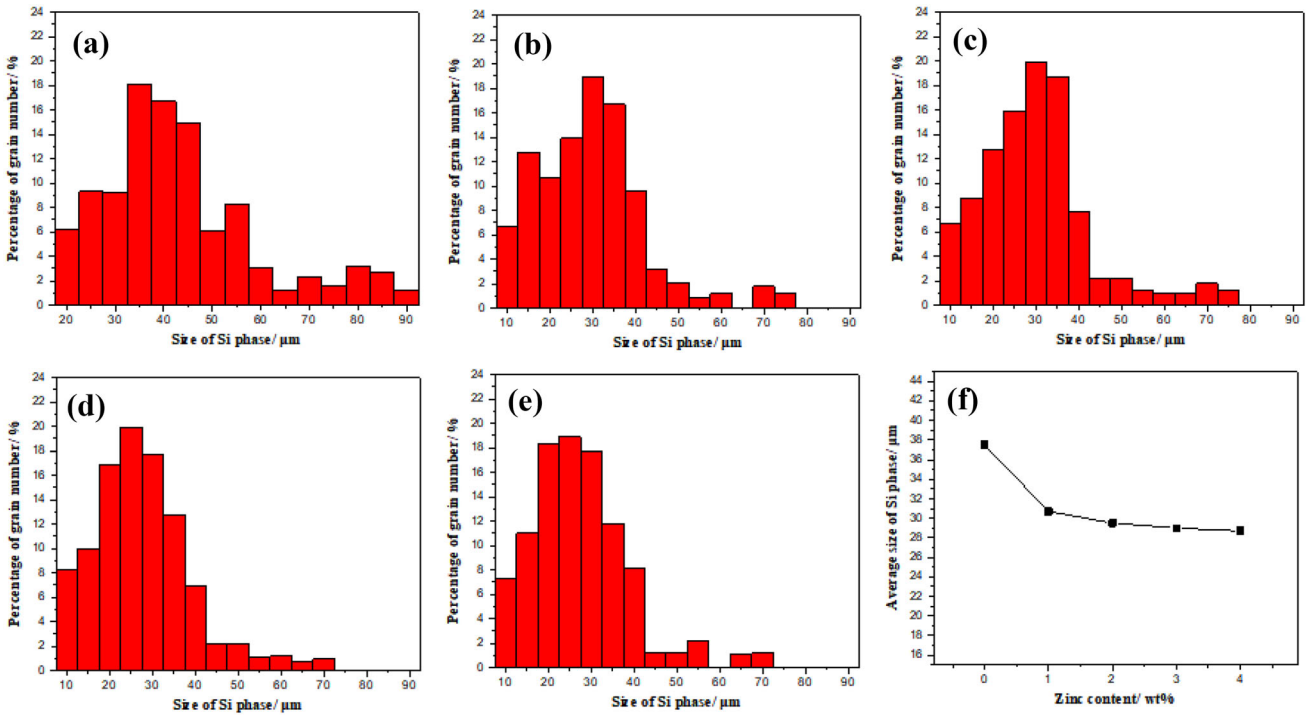

Figure 4. Grain size distribution and average size of the Si phase in alloys with different Zn content: (a) Al-12.5Si-2Cu-1Mg; (b) Al-12.5Si-1Zn-2Cu-1Mg; (c) Al-12.5Si-2Zn-2Cu-1Mg; (d) Al-12.5Si-3Zn-2Cu-1Mg; (e) Al-12.5Si-4Zn-2Cu-1Mg; (f) average size of Si phase.

and Cu in the alloy. According to Reference, the Al-Si-Cu-Mg alloy's phase composition consists mainly of α-Al, α-Al + Si eutectic structure, primary Si phase, θ-Al_2Cu phase, Q-$Al_5Cu_2Mg_8Si_6$ phase and iron-rich phase π-$Al_8Mg_3FeSi_6$ phase.[4] This is inconsistent with the results of the XRD pattern, and more scanning electron microscopy analysis is required.

The enrichment regions of Si, Mg and Cu in Figure 6 (a), (b) and (d) were quantitatively characterized by EDS, and the phases were deduced based on the atomic ratio. The results are listed in Table 2. The primary compound phases of Al-12.5Si-2Cu-1Mg alloy include θ-Al_2Cu phase, Q-$Al_5Cu_2Mg_8Si_6$ phase and the iron-rich phase π-$Al_8Mg_3FeSi_6$, among which the bright white lamellar

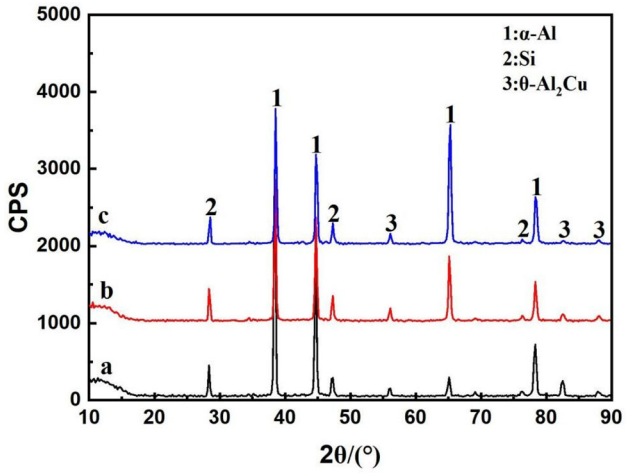

Figure 5. XRD patterns of different alloys (a) Al-12.5Si-2Cu-1Mg; (b) Al-12.5Si-2Zn-2Cu-1Mg; (c) Al-12.5Si-4Zn-2Cu-1Mg.

copper-rich phase is θ-Al_2Cu phase. The Mg-rich phase in the alloy is the Q-$Al_5Cu_2Mg_8Si_6$ phase, and no Mg2Si phase is found, indicating that the Mg element in the alloy mostly forms the Q-$Al_5Cu_2Mg_8Si_6$ phase, which may be a result of the high Cu/Mg ratio in the alloy. Reference[5] has pointed out that Mg_2Si in Al-Si-Mg-Cu alloys decreases with the increase of Cu content, and the Mg_2Si phase disappears after the Cu content reaches a certain value; the Chinese-script-like iron-rich phase is π-$Al_8Mg_3FeSi_6$, which is less damaging to the alloy than the acicular β-Fe phase commonly observed in cast aluminum alloys.

Similar to the alloy without Zn, the main compounds in the alloy with Zn are still θ-Al_2Cu phase, Q-$Al_5Cu_2Mg_8Si_6$ phase and π-$Al_8Mg_3FeSi_6$ phase. Compare to the microstructures in Figure 6 (a) and (b), the morphology of the Q-$Al_5Cu_2Mg_8Si_6$ phase in the alloy containing 2 wt% Zn changes from flake to fishbone when compared to the morphology of the phase in the alloy without Zn. The π-$Al_8Mg_3FeSi_6$ phase contains a minor amount of Mn and changes from Chinese script to strip shape.

In addition, as shown in Figure 7, as the Zn content increases to 4 wt%, the copper-rich phase θ-Al_2Cu transforms from lamellar to irregular small flakes, the phase size reduces, and granular particles appear in the surrounding area.

Effect of Zn Content on Mechanical Properties

As-cast Mechanical Properties

The hardness and mechanical properties of the as-cast Al-12.5Si-xZn-2Cu-1Mg alloy are shown in Figure 8. Without Zn, the as-cast tensile strength of the alloy is 218 MPa. Tensile strength increases initially and then decreases as Zn content in the alloy increases. The maximum tensile strength of the as-cast 2 % Zn alloy is 235 MPa. The

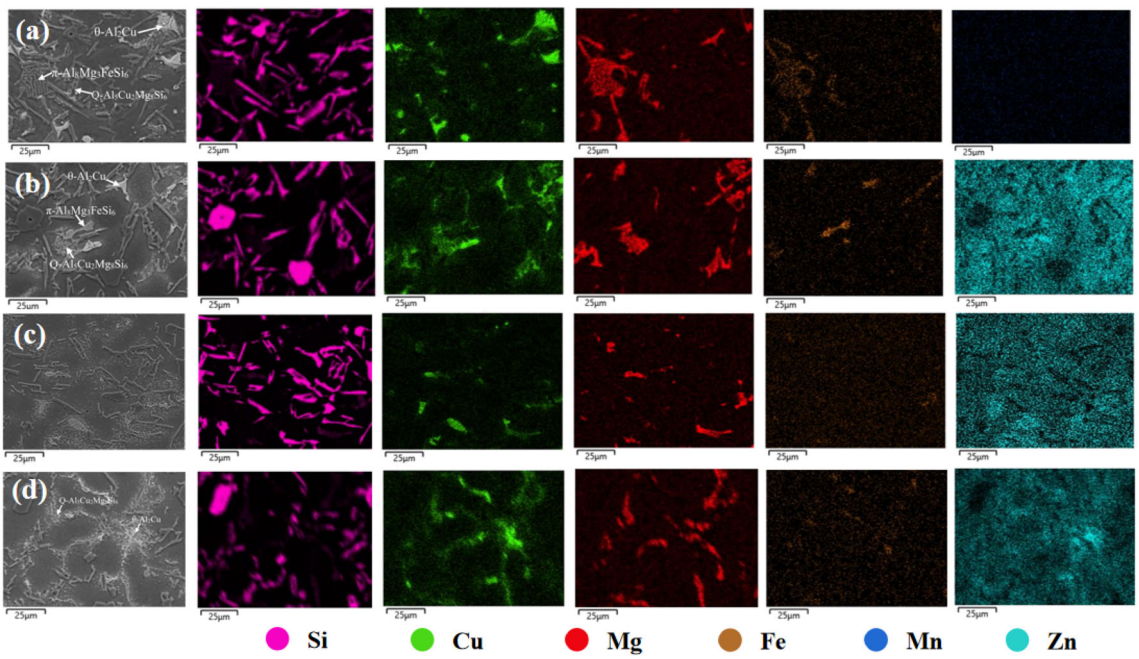

Figure 6. SEM morphology and EDS scanning analysis of different alloys: (a) Al-12.5Si-2Cu-1Mg; (b) Al-12.5Si-2Zn-2Cu-1Mg; (c) Al-12.5Si-3Zn-2Cu-1Mg; (d) Al-12.5Si-4Zn-2Cu-1Mg.

Table 2. Results of Quantitative EDS Analyses of Phases in Figure 6 (a), (b) and (c)

No.	Element (Atom Fraction%)							Phase
	Al	Si	Cu	Mg	Fe	Mn	Zn	
Cu-rich phase in (a)	64.11	4.24	31.65	–	–	–	–	θ-Al_2Cu
Mg-rich phase in (a)	46.98	22.67	9.21	21.15	–	–	–	Q-$Al_5Cu_2Mg_8Si_6$
Fe-rich phase in (a)	69.43	17.33	0.81	9.27	2.94	0.23	–	π-$Al_8Mg_3FeSi_6$
Cu-rich phase in (b)	64.46	4.05	31.49	–	–	–	–	θ-Al_2Cu
Mg-rich phase in (b)	46.98	22.67	9.21	21.15	–	–	–	Q-$Al_5Cu_2Mg_8Si_6$
Fe-rich phase in (b)	70.84	16.19	0.49	9.21	2.68	0.59	–	π-$Al_8Mg_3FeSi_6$
Cu-rich phase in (d)	66.24	1.41	32.35	–	–	–	–	θ-Al_2Cu
Mg-rich phase in (d)	18.02	22.67	10.59	39.49	–	–	0.77	Q-$Al_5Cu_2Mg_8Si_6$

alloy's yield strength and hardness increase as its Zn content rises. Without Zn, the alloy's yield strength and hardness are 142.7 MPa and 90.5 HB, respectively. With a 4 % Zn addition, the alloy's yield strength and hardness increase to 163.2 MPa and 103.0 HB, respectively. The elongation of the alloy reduces as the proportion of zinc increases. In conclusion, the effect of Zn on the mechanical properties of as-cast Al-12.5Si-xZn-2Cu-1Mg alloy can improve the alloy's strength but decrease its plasticity.

T6 Heat-Treated Mechanical Properties

The hardness and mechanical properties of Al-12.5Si-xZn-2Cu-1Mg alloy after T6 treatment are shown in Figure 9. The figure demonstrates that the tensile strength of the Al-12.5Si-xZn-2Cu-1Mg alloy is greatly enhanced after heat treatment compared to the as-cast tensile strength, and that the tensile strength of the alloy after T6 treatment increases with the increase of Zn content in the alloy. After T6 treatment, the alloy with a 4 wt% Zn addition has a yield strength of 378 MPa and a Brinell hardness of 145 HB. The elongation of the alloy after heat treatment is not significantly higher than that of the as-cast alloy, and the elongation decreases as the Zn content of the alloy increases.

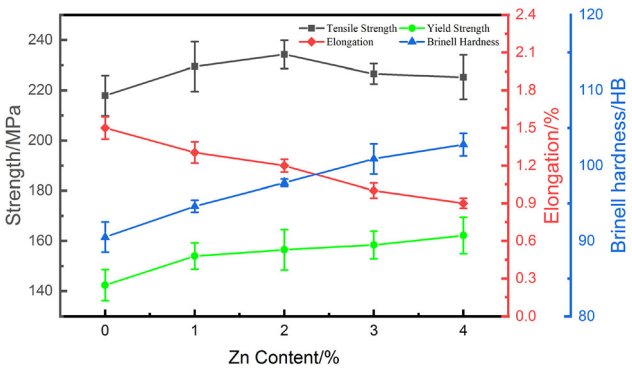

Figure 8. Hardness and mechanical properties of as-cast Al-12.5Si-xZn-2Cu-1Mg alloy.

Friction and Wear Properties

The friction and wear tests of Al-12.5Si-xZn-2Cu-1Mg alloy with different Zn contents were conducted after T6 heat treatment, and the wear resistance was compared to that of ENAC-AlSi12CuNiMg alloy.[16] Figure 10 shows the wear amounts and steady-state average friction coefficients of Al-12.5Si-xZn-2Cu-1Mg alloy and ENAC-AlSi12Cu-NiMg alloy. According to the graph, the mass loss of Al-12.5Si-xZn-2Cu-1Mg alloy during wear reduces as the Zn

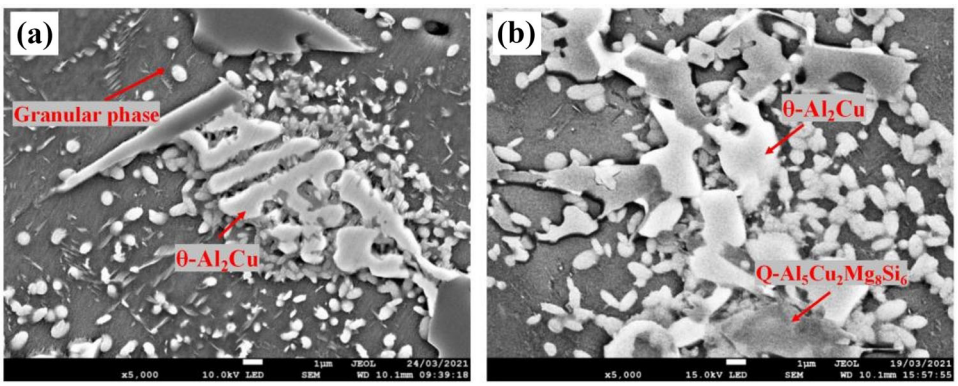

Figure 7. Morphology of θ-Al_2Cu in a high Zn content alloy: (a) Al-12.5Si-3Zn-2Cu-1Mg; (b) Al-12.5Si-4Zn-2Cu-1Mg.

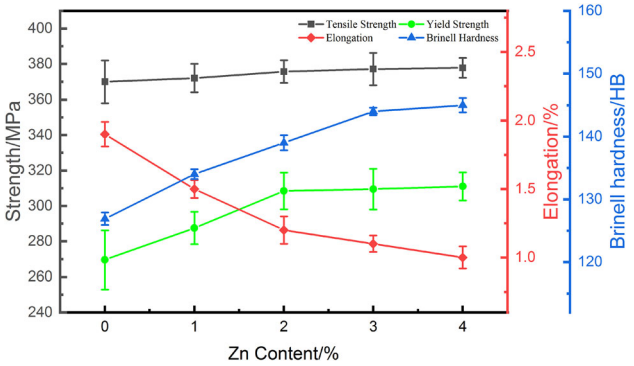

Figure 9. Hardness and mechanical properties of a heat-treated Al-12.5Si-xZn-2Cu-1Mg alloy.

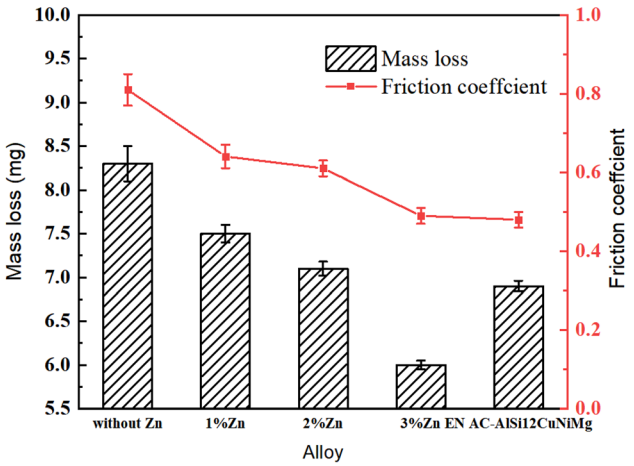

Figure 10. Friction and wear properties of different alloys.

content of the alloy increases. The wear amount of the alloy without Zn element during wear is 8.3 mg. When the Zn content in the alloy is increased to 3 wt%, the wear amount of the alloy reduces to 6 mg, which is less than the ENAC-AlSi12CuNiMg alloy. In addition, as Zn content increases, the friction coefficient of Al-12.5Si-xZn-2Cu-1Mg alloy drops. The friction coefficient of the alloy containing 3 wt% Zn is comparable to that of the EN AC-AlSi12CuNiMg alloy.

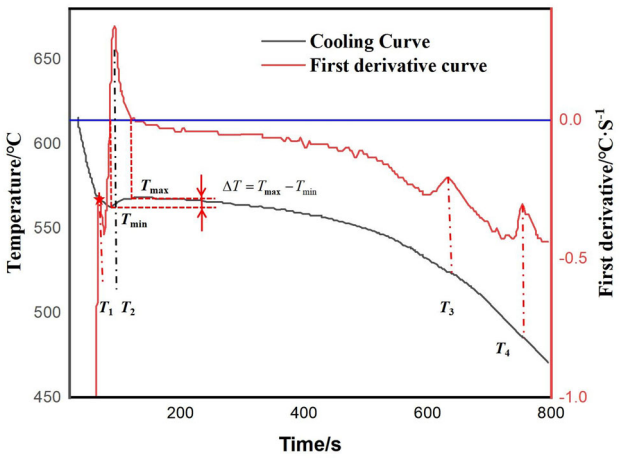

Figure 11. Cooling curves and first order differential curves of Al-12.5Si-2Cu-1Mg alloy

Discussion

Analysis of the Solidification Process and Mechanism of Microstructure Formation

Figure 11 shows the cooling curve of the Al-12.5Si-2Cu-1Mg alloy and the first differential curve that corresponds to it after computer processing. Based on the change rule of the first differential curve, the characteristic points and values on the cooling curve are determined and extracted.

As shown in Figure 11, the differential curve of the alloy exhibits four distinct peaks. Table 3 displays the temperatures corresponding to the four peaks on the cooling curve. The table also lists the temperature value and temperature gap corresponding to the second characteristic peak when the rate of change is 0. The first peak on the differential curve corresponds to the precipitation of primary Si; the second peak corresponds to the α-Al+Si eutectic transformation, as determined by the results of phase and microstructure investigation of the alloy. The eutectic transformation is the main transformation of Al-12.5Si-xZn-2Cu-1Mg alloy solidification. The transformation process releases a large amount of latent heat of crystallization, causing the temperature to rise, that is, the recalescence phenomenon. The third and fourth peaks

Table 3. Characteristic Point Temperature of Al-12.5Si-xZn-2Cu-1Mg Alloy

Item	T_1/°C	T_2/°C	T_3/°C	T_4/°C	T_{min}/°C	T_{max}/°C	△T/°C
Al-12.5Si-2Cu-1Mg	565.9	566.6	536.5	494.4	564.6	569.2	4.6
Al-12.5Si-1Zn-2Cu-1Mg	566.2	565.2	530.1	490.8	564.2	568.3	4.1
Al-12.5Si-2Zn-2Cu-1Mg	566.8	564.5	524.1	485.9	563.9	567.8	3.9
Al-12.5Si-3Zn-2Cu-1Mg	567.3	563.2	519.3	471.2	562.3	567.5	3.2
Al-12.5Si-4Zn-2Cu-1Mg	568.7	562.4	512.5	464.3	561.6	564.5	2.9

represent the transition of alloying elements into a compound phase in the alloy.

The solidification structure of the as-cast Al-12.5Si-2Cu-1Mg alloy is mainly composed of α-Al dendrites, α-Al + Si eutectic structure, block primary Si and θ-Al_2Cu phase according to XRD results. Zn and its compounds are not observed in the microstructure and XRD results of the alloy after adding Zn, indicating that Zn promotes the solid solution of Zn in the aluminum matrix due to its high solubility in α-Al, which is consistent with the results of Zn element surface scanning. In the experiment, P modifier can form AlP with a comparable crystal structure to Si with Al, which can be employed as the nucleation core to promote the non-spontaneous nucleation of the Si phase. The results shown in Table 3 shows that the growth temperature of the primary Si phase increases to 568.7 °C and the intensity of the peak on the corresponding differential curve increases with the increase of Zn content in the alloy. This indicates that the primary Si phase increases with the increase of Zn content in the alloy. In addition, the eutectic transition temperature decreases by 4.4 °C as the Zn content of the alloy increases, which is consistent with the results of the Al-Si-Zn phase diagram[17], and the difference T between the maximum temperature Tmax and the minimum temperature Tmin of the eutectic decreases as the Zn content of the alloy increases. Zhang et al. hypothesized that the eutectic Si phase tends to grow in the {111} Si direction, and that Zn limits the growth of the eutectic Si on the {111} Si surface, forcing the eutectic Si to shift its stacking and therefore inhibiting its growth.[18]

In the alloy composition design, a Cu/Mg mass ratio of 2 was adopted, which not only prevents the formation of the Mg2Si phase by the Mg element, but also guarantees the simultaneous formation of θ-Al_2Cu phase and Q-$Al_5Cu_2Mg_8Si_6$ phase.[5,19] According to the results of phase analysis, the alloy contains less π-$Al_8Mg_3FeSi_6$ phase. Based on the results and conclusion in previous references[4,20], the third peak (T3) corresponds to the reaction being L → Q-$Al_5Cu_2Mg_8Si_6$, and the fourth peak (T4) corresponds to the reaction being mainly L → α-Al + Si + θ-Al_2Cu. T3 and T4 transition temperatures decrease dramatically with increasing Zn content in the alloy, demonstrating that Zn decreases the phase formation temperature of θ-Al_2Cu phase and Q-$Al_5Cu_2Mg_8Si_6$. In addition, the intensity of the third peak on the differential curve increases with the increase of Zn content in the alloy, while the intensity of the fourth peak decreases with the increase of Zn content, indicating that Zn has the effect of promoting the formation of the Q-$Al_5Cu_2Mg_8Si_6$ phase, and the increase in the formation of the Q-$Al_5Cu_2Mg_8Si_6$ phase will reduce the Cu content in the residual liquid phase, leading to the decrease of Cu element through the ternary eutectic reaction to form θ-Al_2Cu, which is also consistent with the previous results that the θ-Al_2Cu phase decreases with the increase of Zn content in the alloy.

In conclusion, the analysis of the solidification process of the Al-12.5Si-xZn-2Cu-1Mg alloy reveals the formation process of the microstructure during the solidification process of the Al-12.5Si-xZn-2Cu-1Mg alloy:

L→L1+ primary Si

L2→L3+ π-$Al_8Mg_3FeSi_6$

L3→L4+ α-Al + eutectic Si

L4→L5+ Q-$Al_5Cu_2Mg_8Si_6$

L5→α-Al+ Si+ θ-Al_2Cu

The Al-12.5Si-xZn-2Cu-1Mg alloy microstructure formation is significantly influenced by the Zn content.

Effect of Zn Content on Mechanical Properties and Wear Resistance of Al-Si-Zn-Cu-Mg Alloy

As shown in Figure 8, as the Zn concentration of the Al-12.5Si-xZn-2Cu-1Mg alloy increases, the tensile strength initially increases and then drops, the yield strength and hardness increase, and the elongation decreases. Tensile strength is the greatest when the zinc content is 2 wt%. With a Zn level of 4 wt%, Brinell hardness is at its maximum. According to the above microstructure and XRD analysis results, this is mainly attributed to the solid solution strengthening effect caused by Zn dissolution in α-Al, the refinement effect of Zn on the Si phase in Al-12.5Si-xZn-2Cu-1Mg alloy, and the reduction in the bulk ternary eutectic θ-Al_2Cu phase, all of which are advantageous for enhancing the strength and hardness of the alloy. With increasing Zn content, however, the tensile strength of the Al-12.5Si-xZn-2Cu-1Mg alloy first increases and subsequently drops. When the alloy's Zn level hits 2 wt%, its tensile strength reaches its maximum value. As the Zn content of an alloy increases, its tensile strength reduces, which may be due to the precipitation of granular Zn-rich phases within the alloy structure. As Zn content increases, the plasticity of the alloy decreases.

The wear surface analysis of the alloy without Zn and with 3 wt% Zn reveals that the wear mechanism includes both adhesive wear and abrasive wear, but the two alloys are distinct in certain respects. Without Zn, the alloy has many adhesive tear pits and severe adhesive wear. The alloy with 3 wt% Zn exhibits reduced adhesive tearing pits and predominantly abrasive wear.[12] Due to the solid solution strengthening effect of Zn on α-Al and the improvement in Si phase size and morphology, an increase in Zn content in the alloy can improve its wear resistance and reduce its friction coefficient.

Conclusion

(1) The as-cast microstructure of Al-12.5Si-xZn-2Cu-1Mg is composed of a small quantity of primary Si, α-Al + eutectic Si, θ-Al_2Cu phase, Q-$Al_5Cu_2Mg_8Si_6$ phase and a small amount of π-$Al_8Mg_3FeSi_6$ phase. In the alloy with a high Zn content, the final solidification zone precipitates a granular Zn-rich phase. Zn influences the size and quantity of the Si phases in the microstructure of the as-cast Al-12.5Si-xZn-2Cu-1Mg alloy. With an increase in the alloy's Zn content, the size of Si phase decreases and the amount of primary silicon increases slightly. The θ-Al_2Cu phase decreases as the Zn content increases.

(2) The as-cast tensile strength of the Al-12.5Si-xZn-2Cu-1Mg alloy increases initially and then decreases as the Zn content in the alloy increases. The 2 wt% Zn alloy has a maximum tensile strength of 235 MPa. The yield strength and hardness of the alloy are enhanced with an increase in the alloy's Zn content, but the alloy's elongation decreases. After T6 heat treatment, the tensile strength, yield strength and hardness increase with the increase of Zn content in the alloy, but the alloy's elongation shows an opposite trend. The addition of Zn improves the alloy's strength and reduces its ductility.

(3) The wear resistance of the Al-12.5Si-xZn-2Cu-1Mg alloy increases as the alloy's Zn content increases. The friction coefficient and mass loss of the alloy decrease as the proportion of zinc increases.

(4) Zn slightly increases the formation temperature of primary Si in Al-12.5Si-xZn-2Cu-1Mg alloy, decreases the eutectic reaction temperature of α-Al + eutectic Si, and greatly reduces the formation temperature of θ-Al_2Cu phase and Q-$Al_5Cu_2Mg_8Si_6$ phase. Zn promotes the formation of Q-$Al_5Cu_2Mg_8Si_6$ phase and reduces the precipitation of θ-Al_2Cu.

Acknowledgements

This work was supported by the Science and Technology Support Program [grant number 2018ZX04027001], Science and Technology Project of Hubei Education Department [grant number Q20211804]. The authors would also like to thank the support of the Analytical and Testing Center, HUAT.

REFERENCES

1. H. Ye, An overview of the development of Al-Si-alloy based material for engine applications[J]. J. Mater. Eng. Perform. **12**(3), 288–297 (2003). https://doi.org/10.1361/105994903770343132
2. H.S. Kang, W.Y. Yoon, K.H. Kim et al., Effective parameter for the selection of modifying agent for Al–Si alloy[J]. Mater. Sci. Eng., A **449**, 334–337 (2007). https://doi.org/10.1016/j.msea.2006.02.363
3. D.K. Dwivedi, Adhesive wear behaviour of cast aluminium–silicon alloys: overview[J]. Mater. Des. **31**(5), 2517–2531 (2010). https://doi.org/10.1016/j.matdes.2009.11.038
4. X. Dong, S. Amirkhanlou, S. Ji, Formation of strength platform in cast Al–Si–Mg–Cu alloys[J]. Sci. Rep. **9**(1), 1–11 (2019). https://doi.org/10.1038/s41598-019-46134-7
5. Y. Zheng, W. Xiao, S. Ge et al., Effects of Cu content and Cu/Mg ratio on the microstructure and mechanical properties of Al–Si–Cu–Mg alloys[J]. J. Alloy. Compd. **649**, 291–296 (2015). https://doi.org/10.1016/j.jallcom.2015.07.090
6. S. Nafisi, R. Ghomashchi, Effects of modification during conventional and semi-solid metal processing of A356 Al-Si alloy[J]. Mater. Sci. Eng., A **415**(1–2), 273–285 (2006). https://doi.org/10.1016/j.msea.2005.09.108
7. S. Gowri, F.H. Samuel, Effect of alloying elements on the solidification characteristics and microstructure of Al-Si-Cu-Mg-Fe 380 alloy[J]. Metall. and Mater. Trans. A. **25**(2), 437–448 (1994). https://doi.org/10.1007/BF02647989
8. S.S. Shin, S.J. Won, H. So et al., High-strength Al-Zn-Cu-Based alloy synthesized by high-pressure die-casting method[J]. Metall. and Mater. Trans. A. **51**(12), 1–10 (2020). https://doi.org/10.1007/s11661-020-06011-9
9. R. Ghiaasiaan, S. Shankar, Effect of alloy composition on microstructure and tensile properties of net-shaped castings of Al–Zn–Mg–Cu alloys[J]. Int. J. Metalcast. **13**, 300–310 (2019). https://doi.org/10.1007/s40962-018-0254-z
10. A.M. Samuel, F.H. Samuel, M.H. Abdelaziz et al., Hardening of Al-Si-Cu-Mg cast alloys: role of Ag and Zn addition. Inter Metalcast **16**, 3–19 (2022). https://doi.org/10.1007/s40962-021-00573-z
11. A.M.A. Mohamed, E. Samuel, A.M. Samuel et al., Effect of intermetallics and tramp elements on porosity formation and hardness of Al-Si-Mg and Al-Si-Cu-Mg alloys. Inter Metalcast (2022). https://doi.org/10.1007/s40962-022-00813-w
12. M.H. Abdelaziz, A.M. Samuel, H.W. Doty, S. Valtierra, F.H. Samuel, Effect of additives on the

microstructure and tensile properties of Al-Si alloys. J. Mater. Technol. **8**, 2255–2268 (2019)
13. S.B. Hwang, B.J. Kim, S.S. Jung et al., Effect of Zn Additions on the mechanical properties of high strength Al-Si-Mg-Cu alloys[J]. J. Korea Foundry Soc. **39**(3), 33–43 (2019). https://doi.org/10.7777/jkfs.2019.39.3.33
14. Y. Nemri, B. Gueddouar, M.E.A. Benamar et al., Effect of Mg and Zn contents on the microstructures and mechanical properties of Al–Si–Cu–Mg alloys[J]. Int. J. Metalcast. **12**(1), 20–27 (2018). https://doi.org/10.1007/s40962-017-0134-y
15. Y. Alemdag, M. Beder, Effects of zinc content on strength and wear performance of Al-12Si-3Cu based alloy[J]. Trans. Nonferrous Metals Soc. China **29**(12), 2463–2471 (2019). https://doi.org/10.1016/S1003-6326(19)65154-X
16. R. Fernandez-Gutierrez, G.C. Requena, The effect of spheroidisation heat treatment on the creep resistance of a cast AlSi12CuMgNi piston alloy[J]. Mater. Sci. Eng., A **598**, 147–153 (2014). https://doi.org/10.1016/j.msea.2013.12.093
17. V. Raghavan, Al-Si-Zn (Aluminum-Silicon-Zinc)[J]. J. Phase Equilib. Diffus. **28**(2), 197–197 (2007). https://doi.org/10.1007/s11669-007-9030-0
18. L.K. Zhang, B.R. Zhang, Effects of Zn on microstructure modification and mechanical properties improvement of Al-Si-Cu-Mg alloys[J]. Metall. Mater. Trans. A. **51**(8), 4158–4167 (2020). https://doi.org/10.1007/s11661-020-05827-9
19. H. Yang, S. Ji, W. Yang et al., Effect of Mg level on the microstructure and mechanical properties of die-cast Al–Si–Cu alloys[J]. Mater. Sci. Eng., A **642**, 340–350 (2015). https://doi.org/10.1016/j.msea.2015.07.008
20. X. Zhu, X. Dong, P. Blake et al., Improvement in as-cast strength of high pressure die-cast Al–Si–Cu–Mg alloys by synergistic effect of Q-$Al_5Cu_2Mg_8Si_6$ and θ-Al_2Cu phases[J]. Mater. Sci. Eng., A **802**, 140612 (2021). https://doi.org/10.1016/j.msea.2020.140612